

EFFECT OF NANOCELLULOSE TYPE AND MATRIX MATERIAL ON
PRODUCTION OF NANOCOMPOSITE FILMS

EKREM DURMAZ and SAIM ATES

*Kastamonu University, Faculty of Forestry, Department of Forest Industrial Engineering,
37150, Kastamonu, Türkiye*✉ *Corresponding author: E. Durmaz, edurmaz@kastamonu.edu.tr**Received February 9, 2023*

The objective of this study has been to investigate the chemical structure, thermal and mechanical properties of nanocomposite films, which were produced by combining cellulose nanofibrils (CNFs) and cellulose nanocrystals (CNCs) with different ratios of boric acid (BA) and polyvinyl alcohol (PVA) as a matrix. Nanocomposites reinforced with BA had B–O–B, and B–O–C ether bonds, while the addition of PVA did not influence the chemical bonds of the films. Furthermore, the addition of BA to CNF and CNC films enhanced the thermal resistance of the films at high temperatures, but the addition of PVA declined the thermal properties of these films. Considering the mechanical properties of nanocomposite films, it was determined that adding PVA to CNF and CNC films had a positive impact, unlike BA. Consequently, it was concluded that each BA and PVA have their advantages and can be preferred for specific industrial applications.

Keywords: cellulose nanofibrils, cellulose nanocrystals, nanocomposites, boric acid, polyvinyl alcohol

INTRODUCTION

The production of novel materials from renewable resources has grown since the early 2000s due to conventional polymers' environmental drawbacks. At the same time, agricultural residues are abundant, and they create an alternative to acquiring added-value products owing to their relatively high cellulose content.¹ Sunflower is among the world's most commonly grown agricultural plants due to its oil and seed. The global production of sunflowers reached 56 million tons, while in Türkiye, it amounted to 2.1 million tons in 2019. Being one of the most cultivated agricultural crops in Türkiye, the cultivation area of sunflower increased by 8.3%, compared to the previous season, and reached about 780 thousand hectares. In addition, 3-7 tons of dry matter per ha of sunflower biomass are obtained annually, which makes these lignocellulosic residues a primary low-cost resource for value-added products, such as different kinds of board, paper, or nanomaterials.²

Cellulose, the most abundant natural polymer on Earth, with about 10^{11} – 10^{12} tons produced annually,³ exhibits great potential and value in manufacturing eco-friendly materials. For many

years, cellulose fibers and their derivatives have been used in the pulp, paper, food, textile, biomedical industries and others.⁴ Nanocellulose, a nano-structured cellulose, can be obtained from various lignocellulosic fibers, and it has attracted the attention of researchers in recent years due to its superior properties. Nanocellulose can be obtained from numerous cellulose sources, such as wood, annual plants, agricultural wastes, bacteria, *etc.* Nevertheless, wood pulp and agricultural residues have been generally preferred in producing nanocellulose.⁵ Nanocellulose has outstanding properties, such as advanced mechanical strength with low density ($1.5\sim 1.6\text{ g/cm}^3$), high surface area ($30\sim 600\text{ m}^2/\text{g}$), high modulus ($100\sim 130\text{ GPa}$), extremely low coefficient of thermal expansion (0.1 ppm/K), superior optical properties, as well as biodegradability and biocompatibility.⁶ Therefore, it has been evaluated for use in composites, coatings, the automotive industry, producing biomedical equipment, energy storage, packaging, paper, water purification, cosmetics, *etc.*^{7,8,9} Nanocellulose is usually classified into two main categories: cellulose nanofibrils (CNFs) and

cellulose nanocrystals (CNCs), depending on the production process and material properties.^{3,6} Cellulose nanofibrils (CNFs), which are produced with a high-shear mechanical treatment, such as high-pressure homogenization, microfluidization, or grinding, have a strong network structure due to their larger dimensions (10–100 nm in diameter, 1–10 µm in length) and the presence of a large number of hydroxyl groups, so they present improved mechanical properties, good thermal stability, excellent biocompatibility, and biodegradability. Meanwhile, cellulose nanocrystals (CNCs), which are obtained via strong acid hydrolysis, exhibit a rod-like structure (5–30 nm in diameter and 100–500 nm in length) with a large specific surface area, better photochemical characteristics, higher crystallinity, and desirable mechanical properties.^{10,11,12}

Many comprehensive studies have focused on using nanocellulose as a reinforcement agent in producing bio-based nanocomposites, for improving the properties of polymer nanocomposites. It has been approved that the reinforcement with nanocellulose has improved some properties, such as mechanical strength, thermal stability, water and oil barrier resistance, optical transparency, and gas permeability.¹³ Unlike inorganic fillers, due to its perfect characteristics, nanocellulose can be extensively used as an organic filler in starch, epoxy resin, waterborne epoxy resin, polyurethane, polyester, rubber, polyolefin, natural polymers, and other polymer composites. Because nonpolar matrixes are poor in interfacial compatibility and indicate weak interaction with polar nanocellulose, different methods, *e.g.*, the modification of either fillers or matrixes or some production processes, have been aimed at improving the compatibility between filler and matrix. In the meantime, owing to the abundance of hydroxyl groups on the surface of nanocellulose, polar nanocellulose demonstrates much better compatibility and adhesion with polar matrixes. Therefore, studies in recent years have focused on the classification of various nanocellulose-filled nanocomposites. Different processes have also been discussed for better dispersion and compatibility of nanocellulose in matrixes of various types.^{14,15,16}

In this study, we primarily aimed to investigate the effects of boric acid (BA) and polyvinyl alcohol (PVA) on the thermal properties and mechanical properties, respectively, of nanocomposite films produced with cellulose nanofibrils (CNFs) and cellulose nanocrystals

(CNCs) obtained from sunflower stalks. We also intended to elucidate the interactions of different nanocellulose types with different matrix types in terms of chemical bonds. For this reason, tensile tests were performed to determine mechanical properties, FTIR analysis – to examine chemical bonds, and TGA analysis – to investigate the thermal behaviour of the nanocomposite films.

EXPERIMENTAL

Materials

In the production of nanocomposite films, polyvinyl alcohol (PVA) and boric acid (BA) were used as matrix materials. PVA and BA were supplied by Akbel Chemistry Company, Türkiye, and Tekkim Chemistry Company, Türkiye, respectively. PVA had 89,000–98,000 M_w , 99+% hydrolyzed, and its viscosity was 20–28 mPa·s. The degree of purity of boric acid was $\geq 99.5\%$. The investigations were carried out in the laboratories of the Department of Forest Industrial Engineering and Mehmet Hakan Akyıldız Central Research Laboratory, Kastamonu University, Türkiye; the Chemical Analysis and Spectroscopy Laboratory (CASL) and other laboratories of the Department of Forest Biomaterials, North Carolina State University, USA; as well as the Wood Mechanics and Technology Laboratory of the Department of Forest Industrial Engineering, Düzce University, Türkiye.

Methods

Production of nanocomposite films

The production and characterization of CNFs and CNCs from bleached sunflower stalk pulp were described in detail in the study of Durmaz and Ates.² Briefly, the grinding process for mechanical disintegration was conducted in CNF production, whereas sulphuric acid hydrolysis was applied as a chemical method in CNC production. The casting method was used in the production of nanocomposite films. The concentrations of CNF and CNC suspensions were 1% and 1.67%, respectively, and these suspensions were treated in an ultrasonic bath for 15 minutes to separate agglomerated nanoparticles. Subsequently, PVA or BA with dimensions in the range of 100–500 µm was added to the nanocellulose suspension in various ratios. These matrixes were dissolved in the suspension for 15–30 min. In the final phase, new suspensions, weighing 80 g total, were processed again in an ultrasonic bath for 15 minutes, and they were made ready for casting in a Teflon mould with a 12 cm diameter and 4 mm thickness. Nanocomposite films were dried in an oven at 60 °C for 1–2 days. The films with PVA or BA took longer to dry than pure nanocellulose films. Besides, at least five films were produced for each sample group with a similar composition.

The solid contents of nanocomposite films produced with CNF, CNC, BA, and PVA were listed in Table 1,

as were the contents of the suspensions, and their corresponding codes between parentheses.

Characterization of nanocomposite films

Fourier transform infrared spectroscopy (FTIR) analysis

Chemical bonds of all film samples were determined by using an FTIR spectrometer (Perkin Elmer Frontier, USA) with a Universal ATR sampling accessory at the Chemical Analysis and Spectroscopy Laboratory, Department of Forest Biomaterials, North Carolina State University, USA. Each sample was scanned twice between 4000 and 650 cm^{-1} wavelengths, with a scanning resolution of 4 cm^{-1} .

Thermogravimetric analysis (TGA)

The thermal properties of all film samples were analyzed with a TGA Q500, TA Instruments, USA, at the Chemical Analysis and Spectroscopy Laboratory, Department of Forest Biomaterials, North Carolina

State University, USA, and with a TGA-DTA Hitachi STA7300 at Mehmet Hakan Akyıldız Central Research Laboratory, Kastamonu University, Türkiye. TGA analysis was conducted under air and nitrogen gas flow at 30–600 $^{\circ}\text{C}$, using a temperature ramp of 10 $^{\circ}\text{C min}^{-1}$.

Mechanical properties

The mechanical properties of the produced film samples were measured with Zwick/Roell Z1.0 1 kN mechanical test equipment according to ASTM D882-10, and as described in the study of Srivastava *et al.*¹⁷ Test were performed on samples with 80 mm x 20 mm dimensions, at a speed of 5 mm/min, at 25 mm gauge length, and with a 1 kN load cell in the Wood Mechanics and Technology Laboratory of the Department of Forest Industrial Engineering, Düzce University, Türkiye.

Table 1
Solid contents of nanocomposite films

CNF/BA	CNC/BA	CNF/PVA	CNC/PVA
100% CNF/0% BA (FB0)	100% CNC/0% BA (CB0)	100% CNF/0% PVA (FP0)	100% CNC/0% PVA (CP0)
67% CNF/33% BA (FB1)	77% CNC/23% BA (CB1)	67% CNF/33% PVA (FP1)	77% CNC/23% PVA (CP1)
50% CNF/50% BA (FB2)	63% CNC/37% BA (CB2)	50% CNF/50% PVA (FP2)	63% CNC/37% PVA (CP2)
40% CNF/60% BA (FB3)	53% CNC/47% BA (CB3)	40% CNF/60% PVA (FP3)	53% CNC/47% PVA (CP3)
33% CNF/67% BA (FB4)	45% CNC/55% BA (CB4)	33% CNF/67% PVA (FP4)	45% CNC/55% PVA (CP4)

RESULTS AND DISCUSSION

All properties of CNFs and CNCs were presented in detail in the study of Durmaz and Ates.² In brief, it was determined by microscopic analysis that CNFs and CNCs had an entangled spaghetti-like structure and a rod-like shape, with high purity. The average width and length of CNCs were found as 13.91 ± 3.09 nm and 60.44 ± 21.06 nm, respectively. In addition, the average width of CNFs was established as 15.03 ± 3.68 nm. The crystallinity index of CNFs and CNCs was confirmed as 82.64% and 83.09%, respectively. It was proposed that although the main thermal degradation stage of CNCs began at a higher temperature than CNFs, the latter were more stable than CNCs at high temperatures. The chemical bonds in CNCs and CNFs were investigated, and the bonds such as O–H, C–H, C–O–C were determined. Besides, the turbidity and zeta potential values of CNFs and CNCs were

found as 14.31 FNU and -38.18 mV for CNFs, as 1.02 FNU and -39.06 mV for CNCs, respectively.

Chemical structure of nanocomposite films

The FTIR results of different types of nanocomposite films are presented in Figure 1. It was observed that the vibrations that form some bonds in 100% CNF and 100% CNC films disappeared proportionally with the increase in the boric acid (BA) ratio in the films. On the other hand, when the bond structures were examined with the addition of boric acid to CNF and CNC suspensions, it was observed that some new peaks appeared in the FTIR spectra. The peak detected at 3338 cm^{-1} in 100% CNF and 100% CNC films indicates free O–H strain in –OH groups, as in the work conducted by Jahan *et al.*¹⁸ The peaks between $3332\text{--}3191 \text{ cm}^{-1}$ and around 1370 cm^{-1} in CNF/BA films are attributed to the hydroxyl groups of boric acid and B–O–B strain vibrations,

respectively. Zhang *et al.*¹⁹ investigated the surface chemistry of modified poplar wood flour in a study that used boric acid as a modification material, and they also found similar results. The weak absorption vibrations observed at 1055 cm⁻¹ and 1029 cm⁻¹ in some CNF/BA and CNC/BA films are thought to be caused by B–O–C strain, similar to the results in the study of Rouhi *et al.*²⁰ The peak around 2900 cm⁻¹ in CNF/BA films reflects C–H strain. Gadhave *et al.*²¹ also determined this type of bond in the same vibration in their study, in which they added boric acid (BA) to the microcrystalline cellulose (MCC)/polyvinyl alcohol (PVA) blend. In addition, it was stated that the peaks in the range of 1422–1407 cm⁻¹ in CNF/BA and CNC/BA nanocomposite films occur due to asymmetric B–O–C strain, as in the work conducted with poly(vinyl alcohol)–borax hybrid foams by Han *et al.*²²

When the results of nanocomposite films with PVA were investigated, it was seen that PVA

added to CNF and CNC suspensions in different ratios inhibited some bond types of 100% CNF and 100% CNC films in the FTIR spectrum. The reason for this is the weak intensity of the peaks detected in 100% CNF and 100% CNC films, and the high permeability of the PVA matrix. The increase in PVA ratios did not change the chemical bonds determined in the FTIR spectra of CNF/PVA and CNC/PVA films; it only affected permeability intensities. Thereby, it was concluded that the chemical bonds of these films were not affected by the change in the PVA ratio. The peak detected at 3338 cm⁻¹ in 100% CNF and 100% CNC films represents the free O–H strain vibration in –OH groups, similar to the results in the work of Jahan *et al.*¹⁸ The peaks observed between 3286 and 3176 cm⁻¹ in CNF/PVA and CNC/PVA films are attributed to typical O–H strain vibrations from intramolecular and intermolecular hydrogen bonds between hydroxyl groups of PVA and nanocellulose, as well as within PVA itself.

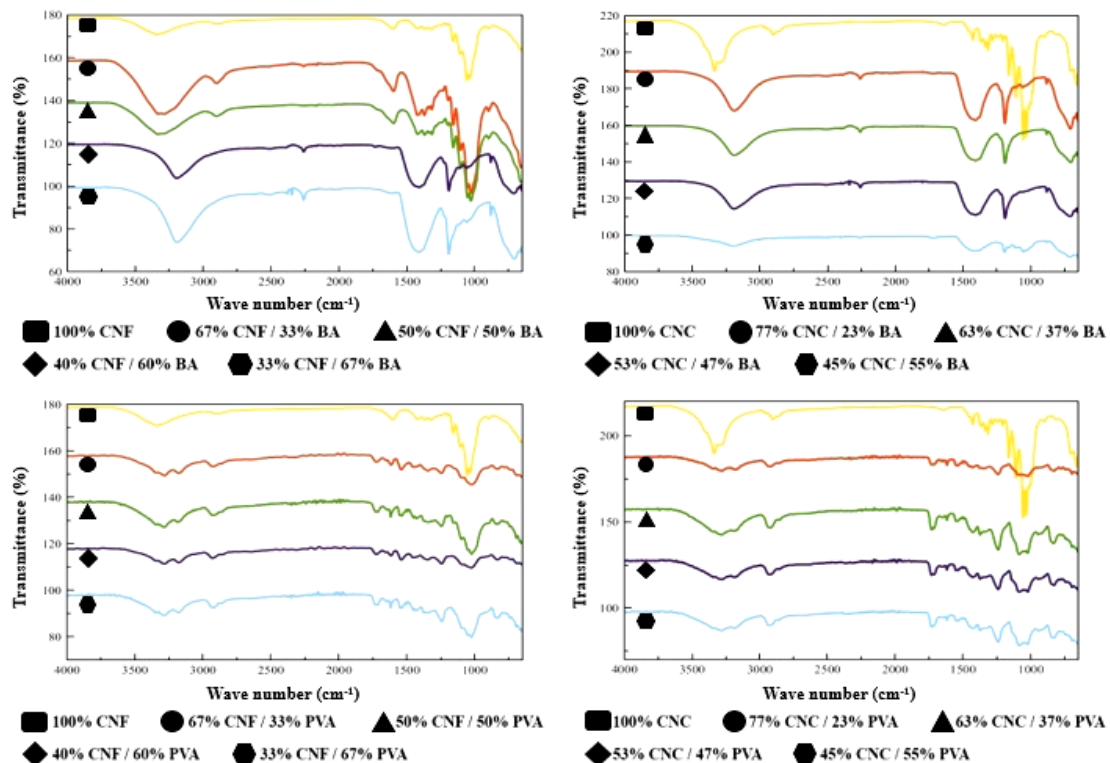


Figure 1: FTIR spectra of nanocomposite films (CNF: cellulose nanofibril, CNC: cellulose nanocrystal, BA: boric acid, PVA: polyvinyl alcohol)

Besides, the peaks determined between 2935–2898 cm⁻¹ are caused by C–H strains of alkyl groups. Mandal and Chakrabarty²³ also found a similar strain in their work, in which they produced nanocomposites based on poly(vinyl alcohol) and nanocellulose obtained from

sugarcane bagasse. The vibrations emerging in the range of 1733–1713 cm⁻¹ in all CNF/PVA and CNC/PVA films indicated C=O and –C–O strains. Similar results were encountered in phosphorylated nanocellulose fibrils (CNF) obtained from bleached softwood kraft pulp/PVA

nanocomposite membranes produced by Niazi *et al.*²⁴

The peaks detected in the ranges of 1452–1428 cm^{-1} and 1374–1316 cm^{-1} reflect the C–H bond, similar to the results in the work of Jahan *et al.*¹⁸ The peak found around 1083 cm^{-1} in CNC/PVA films is the C–O bond. Choo *et al.*²⁵ also confirmed these results in the FTIR analysis of their PVA-chitosan/TEMPO-CNF bio-nanocomposite films. The vibrations that occurred around 834 cm^{-1} in all CNF/PVA and CNC/PVA films were revealed upon the addition of PVA, which supports the interaction of nanocelluloses with the PVA matrix. Peresin *et al.*²⁶ reported similar findings.

Thermal properties of nanocomposite films

The TGA results for nanocomposite films are presented in Figure 2. It was observed that CNF/BA nanocomposite films produced with the addition of BA started to degrade at lower temperatures (between approximately 120–130 °C) compared to 100% CNF film. On the other hand, it was determined that CNF/BA nanocomposites remained more durable at high temperatures (between 450–500 °C) and their weight losses were lesser. Two-stage degradation is seen for BA-added CNF films in Figure 2. The first degradation started at about 130 °C and proceeded to 200 °C, as well as minimum weight loss in this interval was about 10% in FB1 film, while the maximum weight loss was determined to be approximately 30% in FB4 nanocomposite. The second degradation of CNF films with added BA initiated at 200 °C and continued to about 400 °C. Afterward, the degradation continued with a decreasing trend and ended at around 500 °C. As a result, the amount of residual material was 25.03% for FB0 film, 44.06% for FB1 film, 47.40% for FB2 film, 48.17% for FB3 film, and 48.30% for FB4 film. In a similar study, Uddin *et al.*²⁷ investigated the flame retardancy and thermal properties of nanocomposite films produced by using CNF, chitosan, and BA in ratios of 1%, 3%, 5%, 10%, 20%, and 30%. As a result of TGA, it was observed that the highest thermal resistance was in pure chitosan with 30% BA addition and chitosan-CNF films, and the amounts of residual material in these films at 600 °C were found to be 50% for both film types.

In Figure 2, it was observed that CNC/BA films started to degrade at lower temperatures (between approximately 120–130 °C) compared to 100% CNC film. However, it was determined

that CNC/BA nanocomposite films were more resistant at high temperatures (between 450–500 °C) and their weight losses were lower due to the chemical effect of BA. It was confirmed that BA used as a matrix decreased the starting temperatures of the thermal degradation reactions in the films. In contrast, it increased the thermal resistance of the films at high temperatures. The amounts of residual material were 18.44% for CB0 film, 45.43% for CB1 film, 47.72% for CB2 film, 53.78% for CB3 film, and 56.54% for CB4 film. Zhang *et al.*¹⁹ produced composite materials by combining with polyamide pure wood powders and wood powders treated with boric acid in their study, and investigated the thermal properties of chemically modified lignocellulosic materials used in composite production. While the amount of residual material released due to the burning of pure wood powders was found to be approximately 20%, this ratio was determined to be approximately 40% for the amount of residual material released due to the burning of wood powders modified with BA.

It can be seen from Figure 2 that the thermal degradation of 100% CNF and PVA-added CNF nanocomposites started at the same temperature (approximately 250 °C). In addition, the thermal degradation of PVA-added films continued at almost the same temperatures as pure CNF film samples, despite different PVA contents, and ended between 450–500 °C. The point that draws attention here is that the thermal resistance of pure CNF film is higher than the thermal resistance of CNF/PVA nanocomposite films. In other words, the addition of PVA decreased the thermal properties of 100% CNF film due to the chemical structure of PVA. The amounts of residual material in the nanocomposites were found as 25.03% for FP0; 17.80% for FP1; 16.87% for FP2; 13.41% for FP3 and 13.17% for FP4. In a similar study, Lee *et al.*²⁸ investigated the thermal properties of films produced using CNF, CNC, dialdehyde-CNF, dialdehyde-CNC, and PVA. They found that the thermal resistances of PVA/dialdehyde-CNF and PVA/dialdehyde-CNC films were higher than those of PVA/CNF and PVA/CNC films. It was observed that the weight loss of PVA/CNF film was higher than that of pure PVA film, while PVA/CNC film had a similar weight loss to that of the pure PVA film.

In Figure 2, the primary degradation of 100% CNF film is recorded between 290–420 °C. It was determined that the thermal degradation of PVA-added CNC nanocomposites started at lower

temperatures (between 200–300 °C), but continued up to higher temperatures (approximately 480 °C) depending on the PVA content. Besides, since CNC-based nanocomposite films with 47% and 55% PVA started to degrade at higher temperatures, their thermal properties were found to be better than the thermal properties of CNC films with 23% and 37% PVA ratios. However, it was observed that adding PVA at different ratios slightly diminished the thermal properties of CNC films. Similar results were encountered in the study of Niazi *et al.*²⁴ The researchers reported that the thermal properties of the films they produced by combining phosphorylated CNCs were reduced with the addition of PVA. The residual material amounts were calculated as 18.44% for CP0 film, 15.97% for CP1 film, 8.40% for CP2 film, 6.04% for CP3 film, and 5.62% for CP4 film, respectively.

Mechanical properties of nanocomposite films

For the same dry material content, the thicknesses of film samples prepared with CNF and CNC suspensions and different matrix types were determined, and average values are shown in Figure 3. The thickness of pure CNF and pure CNC films was found to be lower than that of

film samples produced adding PVA and BA. According to the figure, the thicknesses of CNF/BA, CNF/PVA, CNC/BA, and CNC/PVA nanocomposite films gradually increased in parallel with the increase in BA and PVA ratios. By mechanical tests, the tensile strength, modulus of elasticity, and elongation at break of CNF-based films were determined. In Figure 4, the tensile strength of 100% CNF films was at its lowest level at 64.87 N/mm² and increased with the addition of PVA. However, increasing PVA concentration harmed the tensile strength of the films and caused it to decrease gradually. Compared to the 100% CNF film, the maximum tensile strength of film FP1 was found to be 85.07 N/mm², which means a 31.13% increase. The highest value in CNF/BA nanocomposites belonged to the 100% CNF film, and the tensile strength of CNF/BA nanocomposite films decreased considerably with the addition of BA. The highest tensile strength value in CNF/BA nanocomposites was 13.88 N/mm² in film FB2. It was concluded that the addition of BA negatively affected the tensile strength of CNF films. Contrary to the addition of PVA, adding BA to the nanocomposite film suspension is most likely producing aggregation issues, because it spreads more homogeneously in CNF nanocomposites.

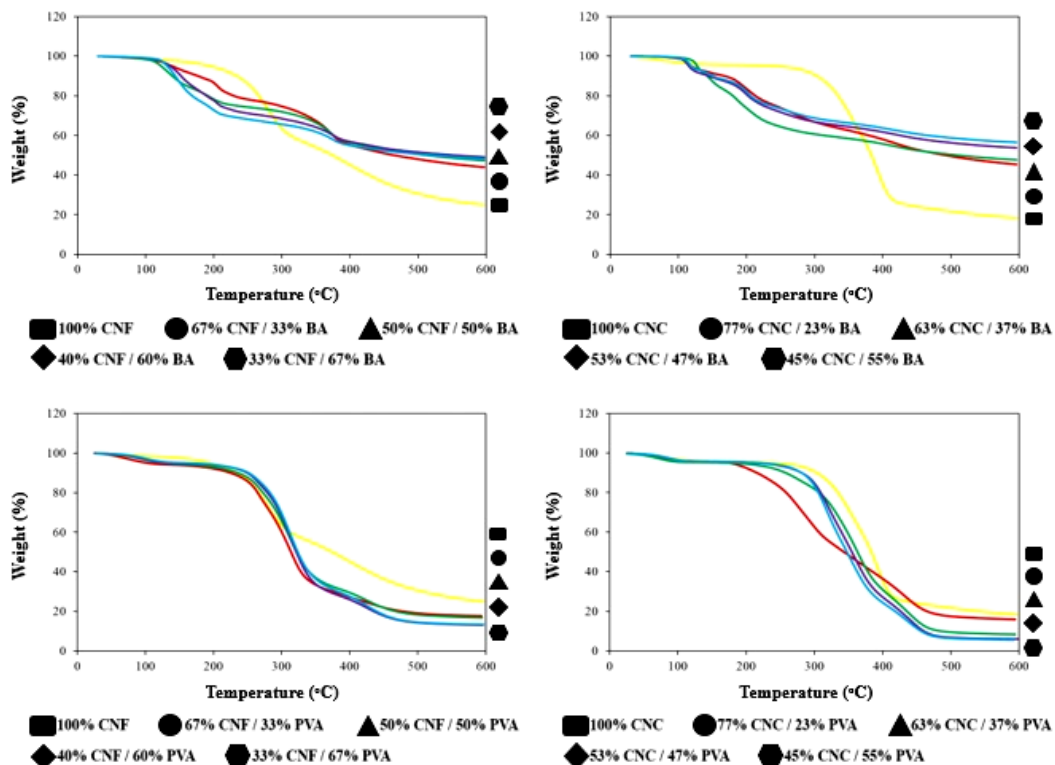


Figure 2: TGA curves of nanocomposite films (CNF: cellulose nanofibril, CNC: cellulose nanocrystal, BA: boric acid, PVA: polyvinyl alcohol)

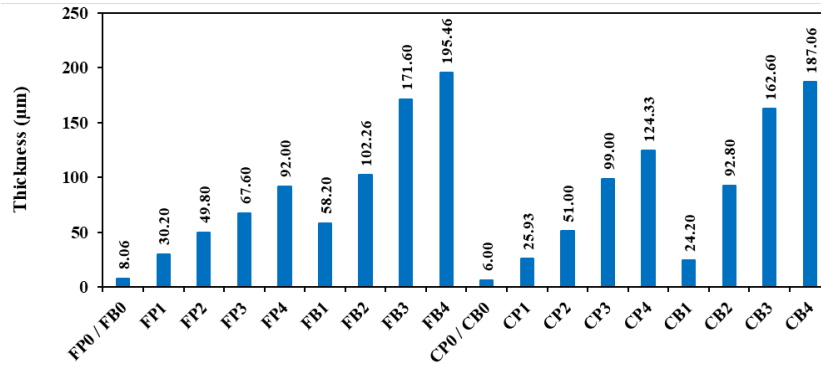


Figure 3: Thickness of nanocomposite films

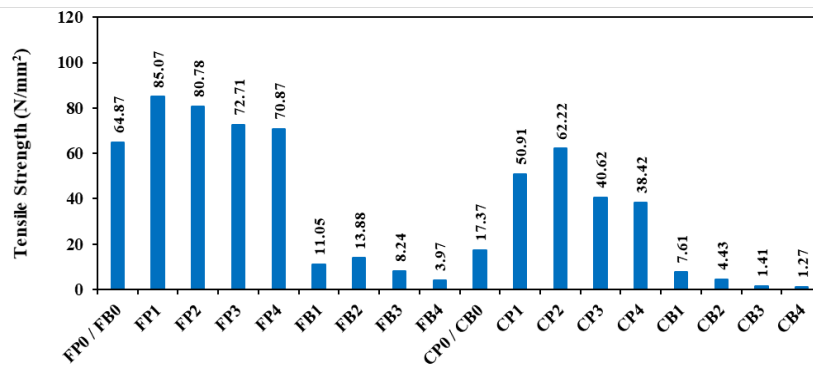


Figure 4: Tensile strength of nanocomposite films

Huang *et al.*²⁹ produced nanocomposite films by combining CNFs obtained from cassava plant wastes with polylactic acid and examined their mechanical properties. At 1% CNF concentration, the greatest tensile strength was determined as 172 MPa; however, at 2% CNF, the tensile strength of nanocomposites decreased to roughly 100 MPa, falling below the tensile strength of pure polylactic acid films. Pavalaydon *et al.*³⁰ obtained cellulose nanocrystal (CNC) from bagasse and coir and used it as a reinforcement agent in PVA-based composites. When the mechanical properties of these films were examined, it was seen that the tensile strength and Young's Modulus of CNC/PVA films were higher than those of pure PVA films. The highest tensile strength was determined as 38.2 ± 0.6 MPa in 0.5% coir CNC/PVA composite, while the highest Young's Modulus was found as 26.4 MPa in 2% sugarcane bagasse CNC/PVA film.

Regarding the tensile strength of CNC-based nanocomposite films, the tensile strength of the pure CNC film was determined to be lower than that of reinforced PVA, and the lowest value was found as 17.37 N/mm². The tensile strength of CNC-based nanocomposites first increased and then tended to reduce with the addition of PVA. The maximum tensile strength in this group was

determined to be 62.22 N/mm², with film CP2 having a 258.20% increase over the pure CNC film. With the addition of BA, tensile strengths of CNC-based nanocomposite films diminished gradually inversely to the increase in BA ratio, and the minimum tensile strength was found as 1.27 N/mm² with a decrease of 92.68% for CB4 nanocomposites compared to the pure CNC film. It was concluded that BA addition negatively affected the tensile strengths of CNC-based films. The reason for this is that PVA disperses more homogeneously in the CNC suspension, contrary to BA, which causes agglomeration problems. Ogunsona and Mekonnen³¹ investigated the mechanical properties of CNC/PVA nanocomposites in their study. PVA films with 3% CNC showed a 125% increase in tensile strength over that of the pure PVA film, whereas films with 10% CNC added to the pure PVA film showed a 321% increase in tensile strength. In another study, Bacha *et al.*³² researched the mechanical characteristics of PVA films reinforced with CNC in different ratios. They found that the tensile strength of composite films increased up to the addition of 5% CNC, and then these tensile strength values declined as CNC concentration increased up to 10%. For adding 5% CNC, the maximum tensile strength of these

films was confirmed as 40.6 ± 0.73 MPa. Moreover, maximum elongation at break was found as 45.7 ± 0.53 % in the composite film with the addition of 2% CNC. Rao *et al.*³³ examined the mechanical properties of coir cellulose nanocrystals (CNC)/oxalic acid (OA)/polyvinyl alcohol (PVA) composite films. With the addition of 3% CNC, the maximum tensile strength and Young's modulus of CNC/PVA films were found as 100.1 MPa and 4272.0 MPa, respectively. Moreover, the highest tensile strength and Young's modulus of OA/PVA films were determined as 125.7 MPa and 4402.3 MPa, respectively, in 30% OA/PVA composites. Considering the maximum tensile strength and Young's modulus of CNC/OA/PVA films, these values were established as 132.4 MPa and 4427.1 MPa, respectively, in 3% CNC/30% OA/PVA composite films.

The modulus of elasticity values of CNF-based films are presented in Figure 5. With the addition of PVA, the modulus of elasticity of CNF-based nanocomposites first of all increased considerably and then gradually decreased. The highest modulus of elasticity was found as 12890.55 N/mm², with an increase of 88.57% in nanocomposite film FP1, compared to the 100% CNF film. In contrast, the lowest modulus of elasticity was established as 6619.24 N/mm² in nanocomposite film FP4. Adding BA in different ratios to CNF films significantly reduced the modulus of elasticity of all films in this group. The modulus of elasticity of CNF/BA nanocomposites gradually lessened with an increase in the concentration of BA matrix. It reduced by 91.71% compared to that of the pure CNF film, and the minimum modulus of elasticity for film sample FB4 was found as 566.23 N/mm². In Figure 5, it was revealed that PVA and BA matrixes added to the film suspensions in increasing ratios made the structures of the

nanocomposite films fragile and considerably reduced their modulus of elasticity. Uddin *et al.*²⁷ determined the highest tensile strength as 325 MPa in chitosan/boric acid films with 20% BA content for chitosan/CNF/boric acid nanocomposite films. On the other hand, in chitosan/CNF/BA films, the tensile strengths of the films increased first with an increase in BA content and reached their highest level with about 275 MPa at 5% BA content. However, the tensile strength of the films decreased gradually at higher BA content (10%, 20%, and 30%) (225 MPa for 10% BA, 200 MPa for 20% BA, and 125 MPa for 30% BA).

The modulus of elasticity of CNC-based nanocomposite films was demonstrated in the same figure. When the modulus of elasticity of CNC/PVA films was examined, it was observed that the addition of PVA decreased the modulus of elasticity of the films. In this group, minimum modulus of elasticity was found as 2513.21 N/mm² for film CP4. A similar situation was seen in CNC/BA nanocomposite films. With an increase in BA concentration, the modulus of elasticity of these films lessened up to 348.61 N/mm² with a reduction of 93.96% compared to the 100% CNC film (for film CB4). When the modulus of elasticity value of the films was examined, it was seen that PVA and BA matrixes added to CNC-based films in increasing ratios made the structures of these films fragile and reduced their modulus of elasticity. When the mechanical properties of the produced nanocomposites were examined in the study of Lani *et al.*,³⁴ the tensile strength of the CNC-free (pure PVA/starch film) film was found as 3.8 MPa. After adding CNC, this value reached the highest level (7.1 MPa) at 10% CNC content, but decreased to 5 MPa and 4.5 MPa, respectively, with a decrease in 15% and 20% CNC content.

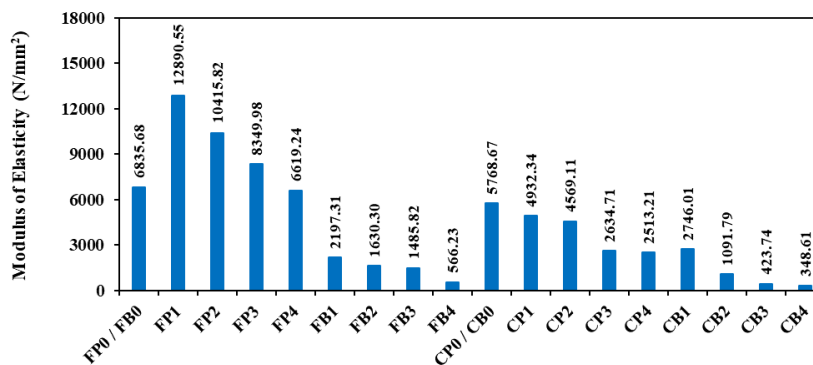


Figure 5: Modulus of elasticity of nanocomposite films

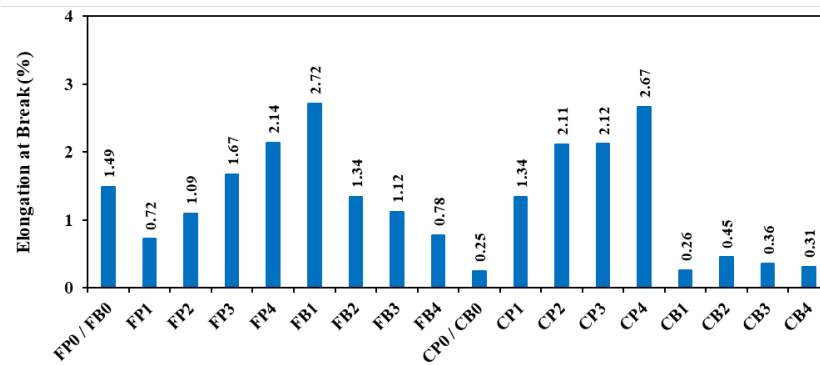


Figure 6: Elongation at break of nanocomposite films

When the elongation values at break of CNF/PVA films were analyzed, the lowest elongation at break value was found as 0.72% for nanocomposite FP1, and the highest elongation value was found as 2.14% for nanocomposite FP4 (Fig. 6). Adding PVA in high ratios increased the elongation at break of the films. The opposite situation was observed with the addition of BA to CNF films. Maximum elongation was found as 2.72% for film FB1, whereas minimum elongation at break was determined as 0.78% for film FB4. Chen *et al.*³⁵ produced starch-based nanocomposite films with CNF obtained from different annual plants and examined their mechanical properties. The maximum tensile strengths were determined as 12.43 MPa for bamboo-CNF at 4% concentration, 10.67 MPa for cotton fiber-CNF at 6% concentration, and 7.67 MPa for sisal-CNF at 8% concentration. Minimum elongation at break values were confirmed as 22.33% for bamboo-CNF at 6% concentration, 23% for cotton-CNF at 10% concentration, and 26.79% for sisal-CNF at 6% concentration.

The addition of PVA to pure CNC films made a positive contribution to the elongation value of the films and as the added PVA ratio increased, the elongation at break values of CNC/PVA films also increased. The nanocomposite CP4 had the largest elongation at break percentage, increasing by 968% as compared to the 100% CNC film. The elongation at break of CNC/BA films increased initially with the increase in added BA content and then showed a decreasing trend. Nonetheless, the elongation values of all CNC/BA nanocomposite films were higher than those of 100% CNC films. The maximum value of elongation at break, which was attained as 0.45% for film CB2, increased by 80% when compared to the value of 100% CNC film. According to

Figure 6, it can be deduced that the addition of high ratios of BA to CNC-based films reduced the mechanical properties by causing agglomeration problems in the films. De Almeida *et al.*³⁶ determined in their study that the highest elongation at break was 62.37% in 1% CNC-added film in standard corn starch nanocomposites. In comparison, the highest elongation at break was found in waxed corn starch nanocomposites as 133.39% in the control sample without CNC. In a different study, Zhang *et al.*³⁷ investigated some mechanical features of different types of PVA-based composite films. In the study, it was confirmed that the native (lignin-cellulose nanocrystals) L-CNCs/PVA film showed a higher Young's modulus and a higher maximum stress at break than the purified (lignin-cellulose nanocrystals) L-CNCs/PVA film and pure PVA. Young's modulus of purified L-CNCs/PVA film diminished, whereas Young's modulus of native L-CNCs/PVA film increased with the addition of L-CNCs to pure PVA. In addition, Young's modulus of the native L-CNCs/PVA film was found to have a maximum value of 3023 MPa. On the other hand, it was seen that native L-CNCs/PVA films had a lower elongation at break (%) than pure PVA and purified L-CNCs/PVA films. Elongation at break was found at about 130% for the pure PVA film, while these values were determined at approximately 70% and 250% for native L-CNCs/PVA and purified L-CNCs/PVA films, respectively.

CONCLUSION

In this research, the properties of nanocomposite films produced with different types of suspensions were examined. Polyvinyl alcohol (PVA) and boric acid (BA) in different ratios were used as matrix agents in cellulose

nanofibril (CNF) and cellulose nanocrystal (CNC) suspensions. FTIR analysis confirmed the chemical bonds that emerge with the addition of PVA and BA, such as B–O–B, B–O–C for BA, and C=O, –C–O for PVA, respectively. In addition, it was found that the thermal stability of nanocomposite films with BA was better than that of pure nanocellulose films and nanocomposite films with PVA. When the mechanical characteristics of nanocomposite films were examined, it was seen that nanocellulose/PVA films had higher tensile strength, modulus of elasticity, and elongation at break than nanocellulose/BA films. Depending on the intended application, both BA and PVA can be preferred for producing nanocomposite films. These films can be evaluated for industrial applications, such as surface coating, food packaging, electronics, and biomedical materials.

ACKNOWLEDGEMENTS: The authors would like to acknowledge the Scientific and Technological Research Council of Türkiye (Türkiye Bilimsel ve Teknolojik Araştırma Kurumu, Project #1059B141800332) for financial support, Dr. Steve Kelley from the Department of Forest Biomaterials, North Carolina State University, for his collaboration and support, the technicians from Chemical Analysis and Spectroscopy Laboratory (CASL) in the Department of Forest Biomaterials, North Carolina State University, and Mehmet Hakan Akyıldız, Central Research Laboratory, Kastamonu University, as well as Dr. Ümit Büyüksarı from the Department of Forest Industrial Engineering, Düzce University, for his support.

REFERENCES

- ¹ S. Ventura-Cruz and A. Tecante, *Food Hydrocoll.*, **118**, 1 (2021), <https://doi.org/10.1016/j.foodhyd.2021.106771>
- ² E. Durmaz and S. Ateş, *Cellulose Chem. Technol.*, **55**, 755 (2021), <https://doi.org/10.35812/CelluloseChemTechnol.2021.55.63>
- ³ O. Nechyporchuk, M. N. Belgacem and J. Bras, *Ind. Crop. Prod.*, **93**, 2 (2016), <https://doi.org/10.1016/j.indcrop.2016.02.016>
- ⁴ T. Rosenau, A. Potthast and J. Hell, "Cellulose Science and Technology: Chemistry, Analysis, and Applications", John Wiley & Sons, 2018, pp. 1-480
- ⁵ S. S. Dalli, B. K. Uprety, M. Samavi, R. Singh and S. K. Rakshit, in "Exploring the Realms of Nature for Nanosynthesis. Nanotechnology in the Life Sciences",

- edited by R. Prasad, A. Jha and K. Prasad, Springer, Cham, 2018, pp. 385-405, https://doi.org/10.1007/978-3-319-99570-0_17
- ⁶ R. J. Moon, A. Martini, J. Nairn and J. Simonsen, *Chem. Soc. Rev.*, **40**, 3941 (2011), <https://doi.org/10.1039/C0CS00108B>
 - ⁷ W. Hamad, *Can. J. Chem. Eng.*, **84**, 513 (2006), <https://doi.org/10.1002/cjce.5450840501>
 - ⁸ L. Brinchi, F. Cotana, E. Fortunati and J. M. Kenny, *Carbohydr. Polym.*, **94**, 154 (2013), <https://doi.org/10.1016/j.carbpol.2013.01.033>
 - ⁹ M. S. Reid, M. Villalobos and E. D. Cranston, *Langmuir*, **33**, 1583 (2017), <https://doi.org/10.1021/acs.langmuir.6b03765>
 - ¹⁰ M. Jonooobi, R. Oladi, Y. Davoudpour, K. Oksman, A. Dufresne *et al.*, *Cellulose*, **22**, 935 (2015), <https://doi.org/10.1007/s10570-015-0551-0>
 - ¹¹ S. H. Osong, S. Norgren and P. Engstrand, *Cellulose*, **23**, 93 (2016), <https://doi.org/10.1007/s10570-015-0798-5>
 - ¹² Y. Hua, T. Chen and Y. Tang, *Ind. Crop. Prod.*, **179**, 1 (2022), <https://doi.org/10.1016/j.indcrop.2022.114686>
 - ¹³ S. P. Bangar and W. S. Whiteside, *Int. J. Biol. Macromol.*, **185**, 849 (2021), <https://doi.org/10.1016/j.ijbiomac.2021.07.017>
 - ¹⁴ A. L. Goffin, J. M. Raquez, E. Duquesne, G. Siqueira, Y. Habibi *et al.*, *Biomacromolecules*, **12**, 2456 (2011), <https://doi.org/10.1021/bm200581h>
 - ¹⁵ A. L. Goffin, J. M. Raquez, E. Duquesne, G. Siqueira, Y. Habibi *et al.*, *Polymer*, **52**, 1532 (2011), <https://doi.org/10.1016/j.polymer.2011.02.004>
 - ¹⁶ J. M. Raquez, Y. Murena, A. L. Goffin, Y. Habibi, B. Ruelle *et al.*, *Compos. Sci. Technol.*, **72**, 544 (2012), <https://doi.org/10.1016/j.compscitech.2011.11.017>
 - ¹⁷ K. R. Srivastava, S. Dixit, D. B. Pal, P. K. Mishra, P. Srivastava *et al.*, *Environ. Technol. Innov.*, **21**, 1 (2021), <https://doi.org/10.1016/j.eti.2020.101312>
 - ¹⁸ Z. Jahan, M. B. K. Niazi and Ø. W. Gregersen, *J. Ind. Eng. Chem.*, **57**, 113 (2018), <https://doi.org/10.1016/j.jiec.2017.08.014>
 - ¹⁹ J. Zhang, A. Koubaa, D. Xing, W. Liu, Q. Wang *et al.*, *Mater. Des.*, **191**, 1 (2020), <https://doi.org/10.1016/j.matdes.2020.108589>
 - ²⁰ M. Rouhi, S. H. Razavi and S. M. Mousavi, *Mater. Sci. Eng. C*, **71**, 1052 (2017), <https://doi.org/10.1016/j.msec.2016.11.135>
 - ²¹ R. V. Gadhave, S. K. Vineeth, P. A. Mahanwar and P. T. Gaddekar, *J. Adhes. Sci. Technol.*, **35**, 1072 (2020), <https://doi.org/10.1080/01694243.2020.1832775>
 - ²² J. Han, Y. Yue, Q. Wu, C. Huang, H. Pan *et al.*, *Cellulose*, **24**, 4433 (2017), <https://doi.org/10.1007/s10570-017-1409-4>
 - ²³ A. Mandal and D. Chakrabarty, *J. Ind. Eng. Chem.*, **20**, 462 (2014), <https://doi.org/10.1016/j.jiec.2013.05.003>

- ²⁴ M. B. K. Niazi, Z. Jahan, S. S. Berg and Ø. Gregersen, *Carbohydr. Polym.*, **177**, 258 (2017), <https://doi.org/10.1016/j.carbpol.2017.08.125>
- ²⁵ K. Choo, Y. C. Ching, C. H. Chuah, S. Julai and N. S. Liou, *Materials*, **9**, 644 (2016), <https://doi.org/10.3390/ma9080644>
- ²⁶ M. S. Peresin, Y. Habibi, J. O. Zoppe, J. J. Pawlak and O. J. Rojas, *Biomacromolecules*, **11**, 674 (2010), <https://doi.org/10.1021/bm901254n>
- ²⁷ K. M. A. Uddin, M. Ago and O. J. Rojas, *Carbohydr. Polym.*, **177**, 13 (2017), <https://doi.org/10.1016/j.carbpol.2017.08.116>
- ²⁸ H. Lee, J. You, H. J. Jin and H. W. Kwak, *Carbohydr. Polym.*, **232**, 1 (2020), <https://doi.org/10.1016/j.carbpol.2019.115771>
- ²⁹ J. Huang, S. Wang, S. Lyu and F. Fu, *Ind. Crop. Prod.*, **122**, 438 (2018), <https://doi.org/10.1016/j.indcrop.2018.06.015>
- ³⁰ K. Pavalaydon, H. Ramasawmy and D. Surroop, *Environ. Dev. Sustain.*, **24**, 9963 (2022), <https://doi.org/10.1007/s10668-021-01852-9>
- ³¹ E. O. Ogunsona and T. H. Mekonnen, *J. Colloid Interface Sci.*, **580**, 56 (2020), <https://doi.org/10.1016/j.jcis.2020.07.012>
- ³² E. G. Bacha, H. D. Demsash, L. D. Shumi and B. E. Debesa, *Adv. Polym. Technol.*, **6947591**, 1 (2022), <https://doi.org/10.1155/2022/6947591>
- ³³ X. Rao, Z. Ou, Q. Zhou, L. Fu, Y. Gong *et al.*, *J. Appl. Polym. Sci.*, **139**, 1 (2022), <https://doi.org/10.1002/app.52361>
- ³⁴ N. S. Lani, N. Ngadi, A. Johari and M. Jusoh, *J. Nanomater.*, **13**, 1 (2014), <https://doi.org/10.1155/2014/702538>
- ³⁵ Q. Chen, Y. Liu and G. Chen, *Cellulose*, **26**, 2425 (2019), <https://doi.org/10.1007/s10570-019-02254-x>
- ³⁶ V. S. de Almeida, B. R. V. Barretti, V. C. Ito, L. Malucelli, M. A. S. C. Ilho *et al.*, *Mater. Res.*, **23**, 1 (2020), <https://doi.org/10.1590/1980-5373-MR-2019-0576>
- ³⁷ Y. Zhang, A. N. M. A. Haque and M. Naebe, *Nanomaterials*, **12**, 1 (2022), <https://doi.org/10.3390/nano12081320>